

2

**AD-A262 293**



OFFICE OF NAVAL RESEARCH

Contract N00014-91-J-1927

R&T Code 413v001

Technical Report No. 19

**DTIC**  
**S ELECTE D**  
MAR 25 1993  
**C**

**STRUCTURE AND THERMODYNAMICS OF THE SOFT ION MODEL  
ELECTROLYTE SOLUTIONS**

by

**LIANRUI R. ZHANG, HENRY S. WHITE, AND H. TED DAVIS**

Prepared for Publication in

**MOLECULAR SIMULATION**

University of Minnesota  
Department of Chemical Engineering and Materials Science  
Minneapolis, MN 55455

March 20, 1993

Reproduction in whole or in part is permitted for any purpose of the United States Government.

This document has been approved for public release and sale; its distribution is unlimited.

**93 3 24 040**

**93-06100**



2108

# REPORT DOCUMENTATION PAGE

Form Approved  
OMB No 2704-0198

Public reporting burden for this collection of information is estimated to average 1 hour per response, including the time for reviewing instructions, searching existing data sources, gathering and maintaining the data needed, and completing and reviewing the collection of information. Send comments regarding this burden estimate or any aspect of this collection of information, including suggestions for reducing this burden, to Washington Headquarters Services, Directorate for Information Operations and Reports, 1215 Jefferson Davis Highway, Suite 1204, Arlington, VA 22202-4302 and to the Office of Management and Budget, Paperwork Reduction Project (2704-0198), Washington, DC 20503.

<b>1. AGENCY USE ONLY (Leave blank)</b>		<b>2. REPORT DATE</b> March 20, 1993	<b>3. REPORT TYPE AND DATES COVERED</b> Technical 6/30/92 - 3/31/93	
<b>4. TITLE AND SUBTITLE</b> STRUCTURE AND THERMODYNAMICS OF THE SOFT ION MODEL ELECTROLYTE SOLUTIONS			<b>5. FUNDING NUMBERS</b> N00014-91-J-1927	
<b>6. AUTHOR(S)</b> LIANRUI R. ZHANG, HENRY S. WHITE, AND H. TED DAVIS				
<b>7. PERFORMING ORGANIZATION NAME(S) AND ADDRESS(ES)</b> Dept. of Chemical Engineering and Materials Science University of Minnesota			<b>8. PERFORMING ORGANIZATION REPORT NUMBER</b> Technical Report No. 19	
<b>9. SPONSORING / MONITORING AGENCY NAME(S) AND ADDRESS(ES)</b> Office of Naval Research 800 North Quincy Street Arlington, VA 22217			<b>10. SPONSORING / MONITORING AGENCY REPORT NUMBER</b>	
<b>11. SUPPLEMENTARY NOTES</b>				
<b>12a. DISTRIBUTION / AVAILABILITY STATEMENT</b> Unclassified/Unlimited			<b>12b. DISTRIBUTION CODE</b>	
<b>13. ABSTRACT (Maximum 200 words)</b>  A soft ion (SI) model of 1:1 electrolytes (0.1 to 5 molar concentration) has been studied by Grand Canonical Monte Carlo (GCMC) simulations and hypernetted chain (HNC) integral equation theory. Pair correlation functions, osmotic pressure, and mean activity coefficients have been calculated as a function of the repulsive soft core potential $r^{-\nu}$ for $\nu = 9$ and 12 (soft ions) and $\nu = \infty$ (hard ions). Results obtained by HNC theory for different electrolyte concentrations and soft core potentials are in excellent agreement with GCMC simulations. At high electrolyte concentration ( $> 1.0$ M), the thermodynamic properties and pair correlation functions of the electrolytes are strongly dependent on $\nu$ . Activity coefficients obtained with a soft core repulsion potential are in good agreement with experimental data for 1:1 electrolytes. Comparison of GCMC results obtained using the minimum image (MI) and Ewald summation methods indicate that the less expensive MI method gives satisfactory results for medium to high electrolyte concentration.				
<b>14. SUBJECT TERMS</b>			<b>15. NUMBER OF PAGES</b> 19	
			<b>16. PRICE CODE</b>	
<b>17. SECURITY CLASSIFICATION OF REPORT</b> Unclassified	<b>18. SECURITY CLASSIFICATION OF THIS PAGE</b> UL	<b>19. SECURITY CLASSIFICATION OF ABSTRACT</b>	<b>20. LIMITATION OF ABSTRACT</b>	

# STRUCTURE AND THERMODYNAMICS OF THE SOFT ION MODEL ELECTROLYTE SOLUTIONS

L. R. Zhang, H. S. White, and H. T. Davis

Department of Chemical Engineering and Materials Science  
University of Minnesota  
Minneapolis, MN 55455

## Abstract

A soft ion (SI) model of 1:1 electrolytes (0.1 to 5 molar concentration) has been studied by Grand Canonical Monte Carlo (GCMC) simulations and hypernetted chain (HNC) integral equation theory. Pair correlation functions, osmotic pressure, and mean activity coefficients have been calculated as a function of the repulsive soft core potential  $r^{-\nu}$  for  $\nu = 9$  and 12 (soft ions) and  $\nu = \infty$  (hard ions). Results obtained by HNC theory for different electrolyte concentrations and soft core potentials are in excellent agreement with GCMC simulations. At high electrolyte concentration ( $> 1.0$  M), the thermodynamic properties and pair correlation functions of the electrolytes are strongly dependent on  $\nu$ . Activity coefficients obtained with a soft core repulsion potential are in good agreement with experimental data for 1:1 electrolytes. Comparison of GCMC results obtained using the minimum image (MI) and Ewald summation methods indicate that the less expensive MI method gives satisfactory results for medium to high electrolyte concentration.

Submitted to Molecular Simulation

Accession For	
NTIS	CRA&I <input checked="" type="checkbox"/>
DTIC	TAB <input type="checkbox"/>
Unannounced <input type="checkbox"/>	
Justification _____	
By _____	
Distribution /	
Availability Codes	
Dist	Avail and/or Special
A-1	

## I. Introduction

The Debye-Hückel (DH) [1] theory of electrolytes has been very successful in describing the structure of dilute electrolytes. The finite size of ions, however, limits the applicability of the DH theory to extremely low ion concentration. One of the most often used models of electrolytes which takes into account the finite size of ions is the primitive model (PM). In this model, the ions interact through a repulsive hard sphere core potential and a Coulomb potential. Systematic investigations of the PM electrolytes using approximate theories and simulations indicate that an oscillatory structure exists in the ion pair correlation functions at high concentrations [3,5,9-13] is not predicted from DH theory.

In a recent report [14], Molecular dynamics (MD) simulations and hypernetted chain (HNC) integral equation theory were used to study the effect of the inverse power law intermolecular repulsion  $1/r^{-\nu}$  (with  $\nu = 4, 6, 9, 12, 24,$  and  $\infty$ ) on the structure of 1:1 electrolytes. Two model systems were investigated. The first (a) is a modified version of the (PM) electrolyte in which all ions were soft spheres and the solvent is represented by a dielectric constant  $\epsilon$ . This model is referred to as the soft ion model (SI). In the second model (b), both ions and solvent molecules were represented by soft spheres and the polar interactions were represented by a dielectric constant  $\epsilon$ . This model is referred to as the soft ion in solution (SIS) model. The results obtained from these investigations indicate that the repulsive interaction potential plays an important role in determining the structural and dynamic properties of electrolytes. For instance, inclusion of the solvent imparted liquid-like structure to the ion-ion pair correlation functions and, for  $\nu \neq \infty$ , gave rise to substantial back scattering oscillations in the velocity autocorrelation functions with a consequent reduction in the particle self diffusion coefficient. Larger values of  $\nu$  reduced the back scattering in the velocity autocorrelation functions. The dynamical behavior of the ions in the SI model is similar to that of the (PM) electrolyte ( $\nu = \infty$ ) when  $\nu \geq 9$ .

In the studies reported here, the thermodynamic properties for SI model of 1:1 electrolytes are obtained from both grand canonical Monte Carlo simulations (GCMC) and HNC theory. Comparison of several physical properties obtained from simulation and theory are used to test the applicability of the HNC theory over a range of electrolyte concentrations. Ionic activity and osmotic coefficients are calculated from simulations and therefore chemical potentials can be obtained. Comparisons of the mean ionic activity coefficients with experimental data for aqueous solutions demonstrate the validity of these soft ion model potentials.

## II. Model systems and Interactions

The studies are carried out for bulk 1:1 electrolytes of ion concentrations ranging from 0.1 to 5 molar. The unit cell for the GCMC simulations is a cubic box of size  $L \times L \times L$  with

periodic boundary conditions in all three dimensions. The interaction potential between ions  $i$  and  $j$  is given by [14]

$$u(r_{ij}) = \frac{A_m |q_i + q_j|}{6\nu d} (d/r)^\nu + \frac{q_i q_j}{\epsilon r_{ij}}, \quad (2.1)$$

where  $d$  is the ion size parameter,  $q_i$  is the ionic charge of species  $i$  (value times the electronic charge),  $\epsilon$  is the dielectric constant (taken to be 78.5), and  $A_m$  is the Madlung constant, equals 1.74,  $\nu$  determines the range of repulsive core interaction. This repulsion comes from the Pauli exclusion principle of the filled electronic shells. For  $\nu = \infty$ , the potential can be written as

$$u(r_{ij}) = \begin{cases} \infty, & r_{ij} < d \\ \frac{q_i q_j}{\epsilon r_{ij}}, & r_{ij} > d. \end{cases} \quad (2.2)$$

which corresponds to primitive model of electrolytes, with a hard core of diameter equal to  $d$ .

### III. HNC Theory

In a bulk electrolyte solution, the structural properties are governed by the Ornstein-Zernike (OZ) equation

$$h_{ij}(r_{12}) = c_{ij}(r_{12}) + \sum_k n_k \int c_{ik}(r_{13}) h_{kj}(r_{32}) dr_3 \quad (3.1)$$

where  $n_k$  is the number density of species  $k$  ( $k = +, -$ ),  $c_{ij}(r_{12})$  and  $h_{ij}(r_{12}) = g_{ij}(r_{12}) - 1$  are the direct and total correlation functions. In the hypernetted chain (HNC) approximation

$$h(r) = c(r) + \ln g(r) + \beta u(r) \quad (3.2)$$

where  $\beta = 1/k_B T$ ,  $k_B$  is the Boltzmann constant and  $T$  is the temperature. The OZ equation becomes [15]

$$\ln y_{ij}(r_{12}) = \sum_k n_k \int [f(r_{13}) y(r_{13}) + y(r_{13}) - 1 - \ln y(r_{13})]_{ik} [(h(r_{32}) + 1) y(r_{32}) - 1]_{kj} dr_3 \quad (3.3)$$

with

$$g(r) = y(r)(f(r) + 1) \quad (3.4)$$

$f(r) = e^{-\beta u(r)} - 1$  is the Mayer function. Using Newton Raphson method with an initial guess for  $y(r)$ , eq.(3.3) is solved with 300 nodes and node spacing of 0.02, and the residue

$$\Delta = \sqrt{\sum_i |y_{i+1} - y_i|^2} \leq 10^{-7}.$$

The excess energy and osmotic pressure are defined as

$$U = 2\pi n \sum_{i=1} \sum_{j=1} x_i x_j \int_0^{\infty} u_{ij}(r) g_{ij}(r) r^2 dr \quad (3.5)$$

and

$$PV/NkT = 1 - \frac{2\pi}{3} n \sum_{i=1} \sum_{j=1} x_i x_j \int_0^{\infty} w_{ij}(r) g_{ij}(r) r^2 dr \quad (3.6)$$

where  $w(r) = r \frac{dw}{dr}$ ,  $x_i$  is the mole fraction of species  $i$ , and  $n$  is the number density with  $n = N/V$ .

#### IV. GCMC Simulations

The Grand canonical ensemble Monte Carlo (GCMC) method was used for all simulations reported herein. The minimum image method (MI) of summing the Coulomb potentials has found to be satisfactory for simulations of a number of ions of  $\sim 100$ . The minimum image method is used through out this work, unless specifically stated, since it is considerably less expensive than the Ewald summation method. In each simulation, the first  $3 \times 10^4$  steps are used to equilibrate the system and the physical properties are calculated from the following equilibrium simulations. The GCMC simulations are performed as following [11,16]: If the probability of accepting a trial step from state  $i$  to state  $j$  is  $f_{ij}$ , then

$$\frac{f_{ij}}{f_{ji}} = \frac{N_i^+! N_i^-!}{N_j^+! N_j^-!} \exp[B - \beta(U_j - U_i)], \quad (4.1)$$

where  $N_i^{\pm}$  and  $N_j^{\pm}$  are the number of cations and anions in states  $i$  and  $j$  and

$$B = 2 [\ln \gamma_{\pm} + \ln(nV)], \quad (4.2)$$

with  $\gamma_{\pm}$  the mean ionic activity. The Markov chain is set up as the following

$$\begin{aligned} f_{ij} &= \min(1, f_{ij}/f_{ji}) \quad \text{addition,} \\ f_{ji} &= \min(1, f_{ji}/f_{ij}) \quad \text{deletion,} \\ f_{ij} &= \min[1, \exp(-\beta U_{ij})] \quad \text{move.} \end{aligned} \quad (4.3)$$

During the simulation, the probability of adding or deleting ions is varied from 0.1- $\frac{1}{3}$ . The starting maximum displacement is  $L/4$  and is adjusted in the first 10000 steps of the simulation such that the probability of accepting a particle move approaches  $\sim 50$  percent if possible. Otherwise the maximum displacement is the value which is fixed at the final adjustment. The number of particles is allowed to fluctuate but the total charge

in the simulation is kept constant. Therefore, at each addition or deletion, a neutral ion pair is added or deleted to maintain charge neutrality. System sizes, the number of steps executed for each simulation, and simulation results are summarized in Tables I-IV.

For the primitive model simulations, the pressure is calculated via the formula

$$PV/NkT = \phi = 1 + U/3NkT + \frac{2\pi nd^3}{3} \sum_i \sum_j x_i x_j g_{ij}(d). \quad (4.4)$$

For simulations of the soft ion model, which has a continuous repulsive potential, the pressure is calculated using the virial theorem

$$\phi = 1 + \frac{1}{3NkT} \left\langle \sum_i r_i \frac{du}{dr_i} \right\rangle. \quad (4.5)$$

## V. Results and Discussions

Simulation and HNC integral equation theory studies of three different core potentials and of different concentrations will be presented in the following. To quantitatively test the applicability of the minimum image method and the system size dependence of simulated thermodynamic properties, simulations with the number of particles from 20 to 216 with MI method, and simulations using Ewald summation and system size of  $N = 64$  were performed for  $\nu = 9$ . The physical properties are given in table I, and the pair correlation functions in figures 1 and 2 for  $C = 1$  molar and 2 molar. For both  $C = 1$  molar and  $C = 2$  molar, the MI method gives pair correlation functions for  $N = 64$  that are in good agreement with results obtained from Ewald sum. The dependence of the pair correlation functions obtained using the MI method on the system size is also shown in figures 1 and 2. The dependence of potential energy and osmotic pressure upon system size  $N$  is much weaker than that of the ionic activity coefficient as demonstrated in Table I. If  $N = 64$  is used in the simulations, the MI method uses considerably less computational time than the Ewald summation. This system size gives a good compromise between accuracy and cost.

Figures 3(a-f) is the calculated and simulated pair correlation functions  $g_{ij}(r)$  of  $\nu = 9$ , for electrolyte concentrations between 0.1 molar to 5 molar. These figures show that the HNC theory is in satisfactory agreement with the GCMC simulations within this concentration range. As the concentration increases, the difference between the like ion pair correlation functions increases slightly. The simulation results show a larger charge inversion at higher concentrations in the second layer than that of HNC. At  $C = 4M$ , there are oscillations evident in the pair correlation functions obtained by both methods.

In figures 4(a-f), one can see even better agreement between the simulated and calculated pair distribution functions for  $\nu = 12$ . Again the oscillations in the pair distribution functions appear at high concentrations for both methods.

Pair correlation functions of the PM obtained by simulation and HNC equation are shown in figures 5(a-f). From these results, it is clear that, the HNC integral equation theory works better for larger steeper core repulsion (large  $\nu$ ). To compare results of the PM and SI models, simulations and HNC calculations of the PM electrolyte using an effective hard sphere diameter  $d = 4.2 \text{ \AA}$  were performed. This diameter is equal to the peak position of  $g_{+-}$  in the SI simulations and is considered to be the effective size of a soft ion. Comparisons between results of ions which have the same effective size are believed to be more meaningful. Still, the rough similarity between the pair distribution functions obtained from the two models exist only at fairly low concentrations, figures 6(a-d). At higher concentration, the PM and SI models give very different results.

Theoretical investigations show that the Debye-Hückel theory breaks down at  $\kappa d \sim 1$  [3-5,9-10] for the PM, where  $\kappa$  is the inverse Debye-Hückel (DH) screening length

$$\kappa = \sqrt{\frac{4\pi \sum_i q_i^2 n_i}{\epsilon kT}}$$

At ion concentration of  $C = 0.1 \text{ M}$ , the DH and HNC theories give almost identical results. At  $C = 5 \text{ M}$  the DH gives an unlike ion pair correlation function peak is about 22% less than that obtained from HNC theory. The simulation results in figures 5(e-f) show a charge inversion which is not predicted from the DH theory. From Table III, we conclude that the onset of the oscillations is consistent with the predictions of  $\kappa d \sim 1$  [4].

The thermodynamic properties gives a much clearer picture of the dependence of the SI model on the steepness of the core repulsion potential, figures 7-9 and Tables I-IV. At infinite electrolyte dilution, all three model potentials ( $\nu = 9, 12, \infty$ ) give the same osmotic pressure and potential energy as well as the same ionic activity. This is the correct ideal gas limit. At finite concentration, the thermodynamic properties are a strong function of  $\nu$ . In figure 9, a comparison is made of simulated ionic activity coefficients with experimental values of several 1:1 electrolytes [17-18]. The mean approach of ions is  $\sim 4.0 \text{ \AA}$  for most of these salts. Given the crude description of the core repulsions, the soft ion model gives very good description of the ionic activity of these salts. Using the PM and the same ionic size parameter, the results are not too bad for KCl. However, the results obtained from the PM seem too steep to characterize most of the salts.

## References

1. Von P. Debye and E. Hückel, *Physik. Z.*, **24**, 185 (1923).
2. J. E. Mayer, *J. Chem. Phys.*, **18**, 1426 (1950).
3. J. C. Rasiyah and H. L. Friedman, *J. Chem. Phys.*, **48**, 2742 (1968); J. C. Rasiyah and H. L. Friedman, *J. Chem. Phys.*, **50**, 3965 (1968); J. C. Rasiyah, *J. Chem. Phys.*, **56**, 3071 (1972).
4. J. G. Kirkwood, *Chem. Rev.*, **19**, 275 (1936); J. G. Kirkwood and J. C. Poirier, *J. Phys. Chem.*, **58**, 591 (1954).
5. F. H. Stillinger and R. Lovett, *J. Chem. Phys.*, **48**, 3858 (1968). R. Lovett and F. H. Stillinger *J. Chem. Phys.*, **48**, 3869 (1968).
6. A. R. Allnatt, *Mol. Phys.*, **8**, 533 (1970).
7. E. W. Waisman and J. L. Lebowitz, *J. Chem. Phys.*, **56**, 3086 (1972).
8. L. Onsager, *Chem. Rev.*, **13**, 73 (1933).
9. C. W. Outhwaite, *Chem. Phys. Lett.*, **5**, 77 (1970). *J. Chem. Phys.*, **50**, 2277 (1969).
10. D. M. Burley, V. C. L. Hutson, and C. W. Outhwaite, *Chem. Phys. Lett.*, **9**, 109 (1971).
11. D. N. Card and J. P. Valleau, *J. Chem. Phys.*, **52**, 6232 (1970). J. P. Valleau and L. K. Cohen, *ibid.*, **72**, 5935 (1980). J. P. Valleau, L. K. Cohen, and D. N. Card, *ibid.*, **72**, 5942 (1980).
12. D. M. Heyes, *Chem. Phys.* **69**, 155 (1982).
13. S. H. Suh, L. Mier-y-Teran, H. S. White, and H. T. Davis, *Chem. Phys.* **142**, 203 (1990).
14. L. R. Zhang, M. Jinno, H. T. Davis, and H. S. White, *submitted to Mol. Simul.*
15. J. A. Barker and D. Henderson, *Rev. Mod. Phys.*, **48**, 587 (1976).
16. L. R. Zhang, H. T. Davis, and H. S. White, *submitted to J. Chem. Phys.*
17. H. S. Harned and B. B. Owen, *The Physical Chemistry of Electrolytic Solutions*, Third edition, Reinhold Book Corporation, New York, 1957.
18. J. E. Zemaitis, D. M. Clark, M. Rafal, and N. C. Scrivner, *Handbook of Aqueous Electrolyte Thermodynamics: theory and applications*, American Institute of Chemical Engineers, New York, 1986.

## Acknowledgements

The support from the Minnesota Supercomputer Institute (MSI), the National Science Foundation, and the Office of Naval Research for this work is gratefully appreciated.

## Figure Captions

- Figure 1. Variation of the pair distribution function of the soft ion model 1:1 electrolyte ( $\nu = 9$ ) as a function of the simulation cell sizes ( $N$  is the number of particles).  $C = 1$  molar. Unless specified, the simulation is done by using minimum image (MI). Keys :  $N = 20$ , (o) for (+-), (●) for (++);  $N = 64$ , ( $\Delta$ ) for (+-), ( $\nabla$ ) for (++);  $N = 216$ , (+) for (+-),  $\times$  for (++);  $N = 64$  using Ewald summation, (—) for (+-), (---) for (++).
- Figure 2. Variation of the pair distribution function of the soft ion model 1:1 electrolyte ( $\nu = 9$ ) as a function of the simulation cell sizes ( $N$  is the number of particles).  $C = 2$  molar. Unless specified, the simulation is done by using minimum image (MI). Keys :  $N = 20$ , (o) for (+-), (●) for (++);  $N = 64$ , ( $\Delta$ ) for (+-), ( $\nabla$ ) for (++);  $N = 216$ , (+) for (+-),  $\times$  for (++);  $N = 64$  using Ewald summation, (—) for (+-), (---) for (++).
- Figure 3. Comparison of pair distribution functions for the soft ion model 1:1 electrolyte for  $\nu = 9$  and  $d = 2.8 \text{ \AA}$  obtained from GCMC simulations and those from HNC integral equation theory. Keys : *GCMC*, (o) for (+-), (●) for (++); *HNC*, ( $\cdots$ ) for (+-), (---) for (++).
- Figure 4. Comparison of pair distribution functions for the soft ion model 1:1 electrolyte for  $\nu = 12$  and  $d = 2.8 \text{ \AA}$  obtained from GCMC simulations and those from HNC integral equation theory. Keys : *GCMC*, (o) for (+-), (●) for (++); *HNC*, ( $\cdots$ ) for (+-), (---) for (++).
- Figure 5. Comparison of pair distribution functions for the PM model 1:1 electrolyte from GCMC simulations and the HNC integral equation theory ( $d = 2.8 \text{ \AA}$ ). Keys : *GCMC*, (o) for (+-), (●) for (++); *HNC*, ( $\cdots$ ) for (+-), (---) for (++).
- Figure 6. Comparison of pair distribution function of the soft ion model 1:1 electrolyte ( $\nu = 9$ ,  $d = 2.8$ , and  $\nu = \infty$ ,  $d = 4.2$ ) obtained from GCMC simulations with HNC results for the primitive model 1:1 electrolyte with an effective diameter  $d = 4.2 \text{ \AA}$  ( $\nu = \infty$ ). Keys : *GCMC*,  $\nu = \infty$ ,  $d = 4.2$ , (o) for (+-), (●) for (++); *GCMC*,  $\nu = 9$ ,  $d = 2.8$ , (---) for (+-), (—) for (++). *HNC*,  $\nu = \infty$ ,  $d = 4.2$ , ( $\cdots$ ) for (+-), ( $\cdots$ ) for (++).

Figure 7. Osmotic coefficients  $\phi$  for a 1:1 electrolyte with  $\nu = 9, 12,$  and  $\infty$  as a function of the concentration. Lines for GCMC, points for HNC.

Figure 8. Potential energy  $U$  for a 1:1 electrolyte with  $\nu = 9, 12,$  and  $\infty$  as a function of the concentration. Lines for GCMC, points for HNC.

Figure 9. Comparison of ionic activity coefficient ( $\ln \gamma_{\pm}$ ) for 1:1 electrolyte ( $\nu = 9, 12,$  and  $\infty$ ) as a function of the concentration with experimental results. The curve corresponding to  $d_e$  is from simulations using an effective ionic radius  $d_e = 4.2 \text{ \AA}$  for  $\nu = 9$ .

Table I. Parameters and results of the HNC calculations and GCMC simulations of a 1:1 electrolyte at different concentrations,  $\nu = 9$ . The side length of the cubic simulation box is  $L$ , the average number of ions is  $\langle N \rangle$ ,  $U$  is the average potential energy,  $C$  is the bulk ionic concentration in molar,  $N_s$  is the number of steps run in the simulation,  $\phi$  is the osmotic coefficient, and  $\gamma_{\pm}$  is the ionic activity,  $B$  is the input parameter.

$L(\text{\AA})$	$B$	$\langle N \rangle$	$-U/NkT$		$\phi$		$C(M)$	$\ln \gamma_{\pm}$	$N_s$ $10^5$
			MC	HNC	MC	HNC			
81.0	6.410	63.87	0.278	0.274	0.933	0.935	0.100	-0.259	5
81.00 <sup>e</sup>	6.413	64.23	0.278		0.933		0.100	-0.263	20
47.37	6.203	63.24	0.453	0.455	0.947	0.948	0.494	-0.352	5
47.37 <sup>e</sup>	6.227	64.10	0.454		0.948		0.501	-0.353	20
25.51	3.978	20.59	0.549	0.536	1.004	1.007	1.029	-0.3424	5
29.84	4.905	32.18	0.540		1.003		1.006	-0.3257	5
37.60	6.345	65.30	0.534		1.008		1.020	-0.3131	2
47.37	7.678	127.38	0.527		1.006		0.995	-0.3152	1
56.39	8.744	215.09	0.525		1.006		0.996	-0.3058	1
37.60 <sup>e</sup>	6.279	63.44	0.531		1.003		0.991	-0.317	20
20.25	4.345	20.38	0.619	0.595	1.154	1.158	2.038	-0.1489	10
23.68	5.301	32.39	0.603		1.153		2.024	-0.1342	3
29.84	6.691	64.22	0.592		1.154		2.007	-0.1232	2
37.60	8.078	125.51	0.585		1.149		1.961	-0.1002	1
44.76	9.124	213.73	0.582		1.154		1.979	-0.1094	1
29.84 <sup>e</sup>	6.671	63.49	0.592		1.151		1.984	-0.122	20
29.84	9.350	128.37	0.578	0.586	1.554	1.564	4.012	0.5133	2
23.68 <sup>e</sup>	7.958	64.42	0.586		1.552		4.026	0.507	20
29.84	10.624	160.98	0.535	0.545	1.807	1.823	5.031	0.9239	3

<sup>e</sup> Ewald sum method is used.

Table II. Same as in Table I with  $\nu = 12$

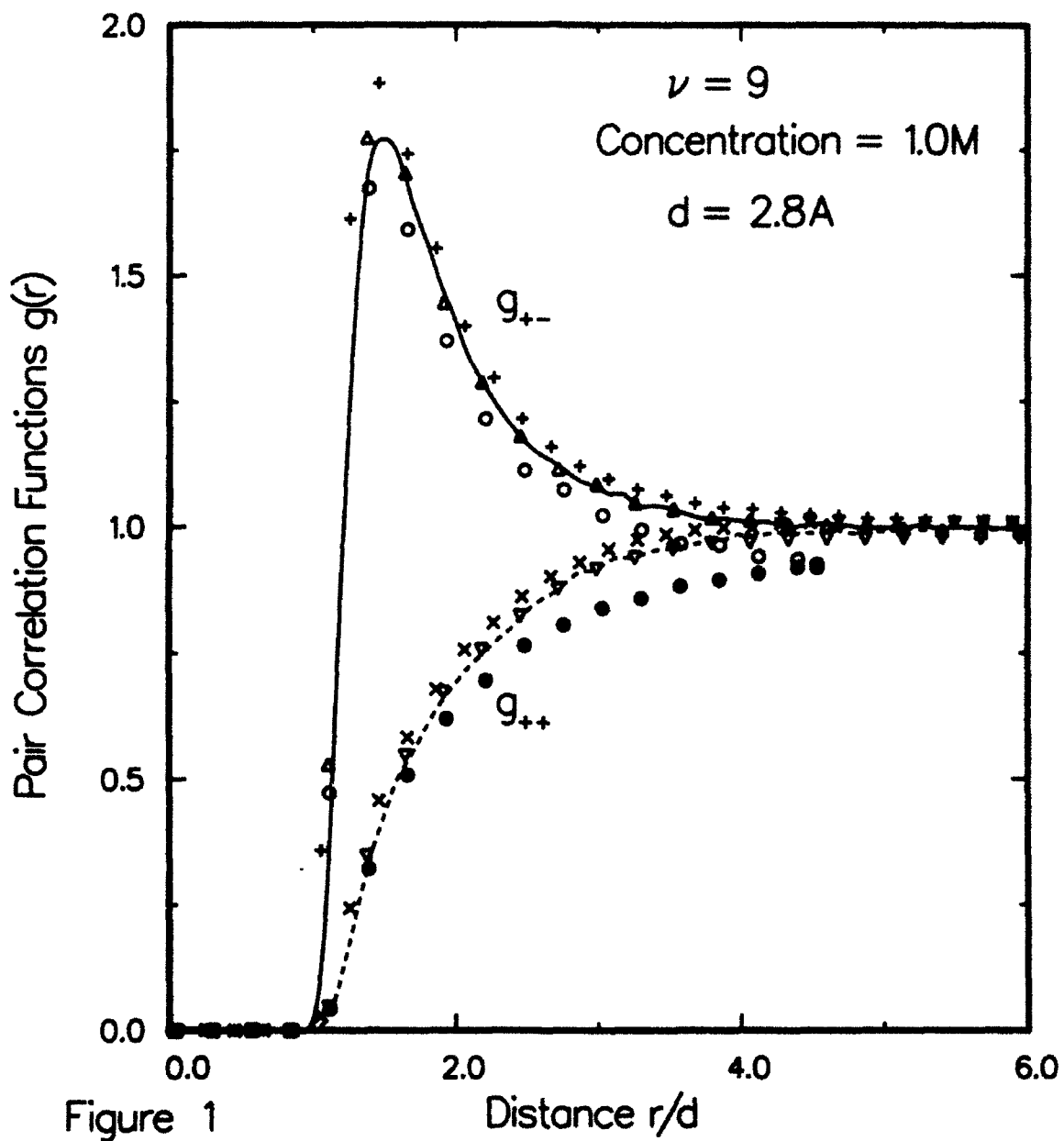
$L(\text{\AA})$	$B$	$\langle N \rangle$	$-U/NkT$		$\phi$		$C(M)$	$\ln \gamma_{\pm}$	$N_s$ $10^5$
			MC	HNC	MC	HNC			
81.0	6.410	65.83	0.292	0.289	0.926	0.927	0.103	-0.2889	2
47.37	6.118	63.81	0.486	0.489	0.922	0.923	0.498	-0.4035	2
37.60	6.142	65.41	0.584	0.591	0.957	0.959	1.022	-0.4167	2
29.84	6.288	63.63	0.674	0.681	1.049	1.054	1.988	-0.3162	2
29.84	8.379	126.56	0.734	0.748	1.304	1.309	3.955	0.0419	2
29.84	9.421	162.94	0.740	0.754	1.481	1.493	5.092	0.3103	2

Table III. Same as in Table I with  $\nu = \infty$  and  $d = 2.8 \text{ \AA}$ .

$L(\text{\AA})$	$B$	$\langle N \rangle$	$-U/NkT$		$\phi$		$C(M)$	$-\ln \gamma_{\pm}$	$N_s$ $10^5$	$\kappa d$
			MC	HNC	MC	HNC				
81.0	6.351	64.60	0.313	0.307	0.912	0.918	0.101	0.299	3	0.2919
47.37	5.931	63.68	0.547	0.542	0.877	0.889	0.497	0.495	3	0.6475
37.60	5.835	64.93	0.676	0.671	0.881	0.896	1.015	0.563	3	0.9253
29.84	5.771	64.90	0.815	0.809	0.913	0.936	2.028	0.594	3	1.3079
29.84	7.366	128.27	0.958	0.956	1.019	1.050	4.008	0.478	4	1.8387
29.84	7.971	15.11	1.006	1.004	1.078	1.115	4.941	0.384	4	2.0413

Table IV. Same as in Table I with  $\nu = \infty$  and  $d = 4.2 \text{ \AA}$ .

$L(\text{\AA})$	$B$	$\langle N \rangle$	$-U/NkT$		$\phi$		$C(M)$	$\ln \gamma_{\pm}$	$N_s$ $10^5$
			MC	HNC	MC	HNC			
81.0	6.451	63.92	0.274	0.270	0.942	0.944	0.100	-0.2388	2
47.37	6.415	65.29	0.464	0.458	0.979	0.989	0.510	-0.2783	2
37.60	6.611	64.33	0.560	0.553	1.079	1.084	1.005	-0.1651	2
32.14	7.384	64.59	0.671	0.659	1.320	1.345	2.019	0.2172	2



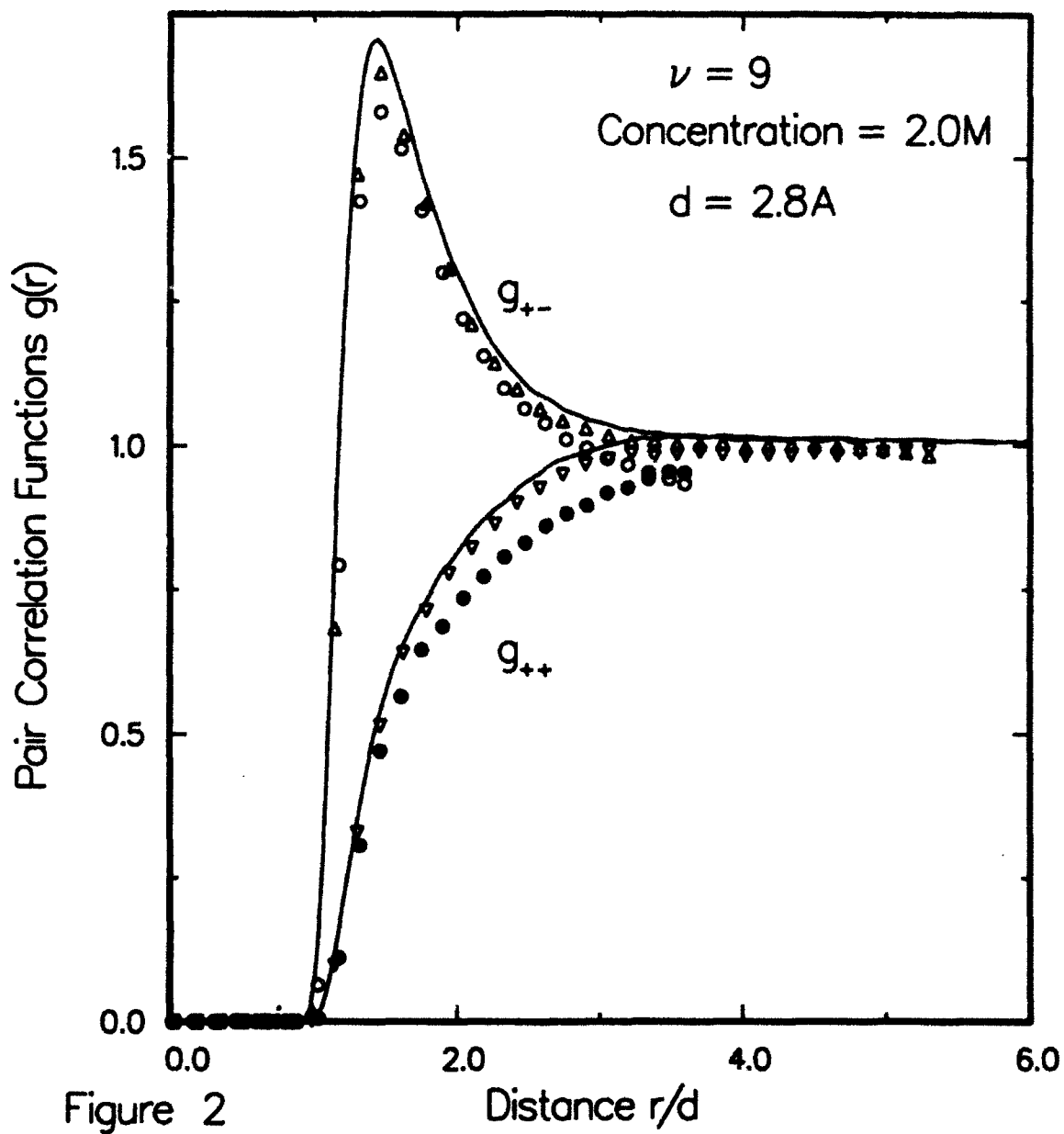


Figure 2

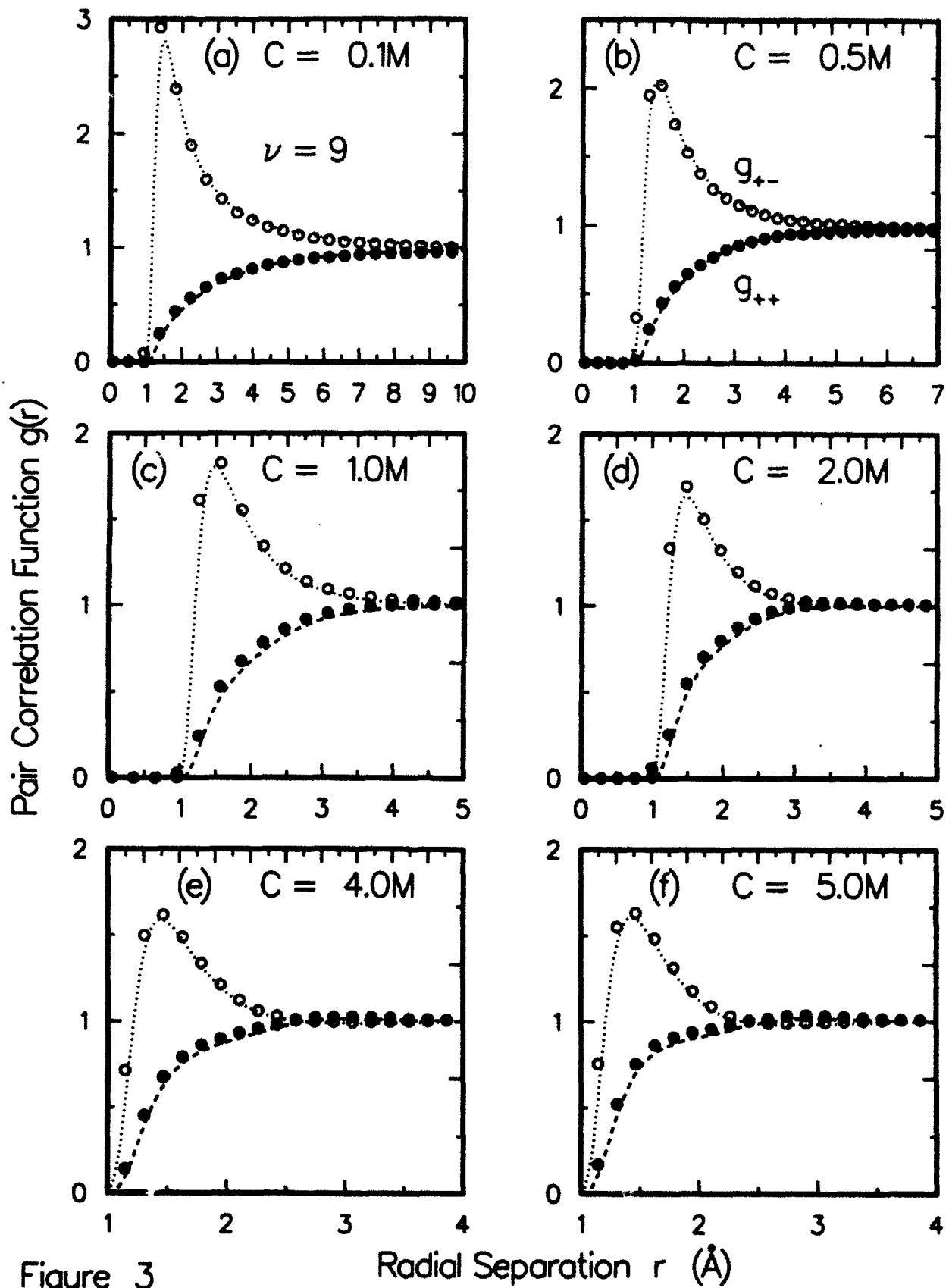


Figure 3

Radial Separation  $r$  (Å)

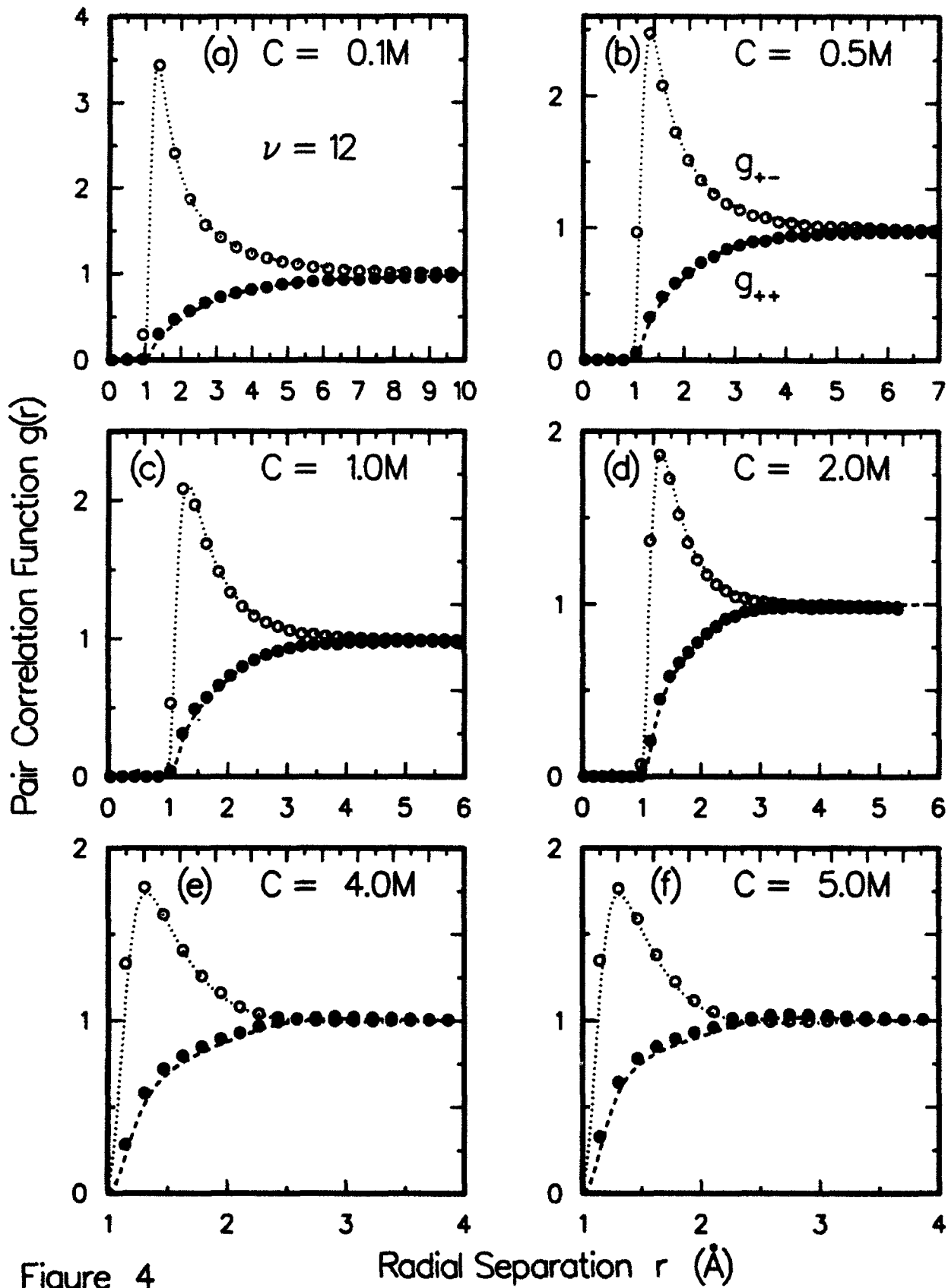


Figure 4

Radial Separation  $r$  (Å)

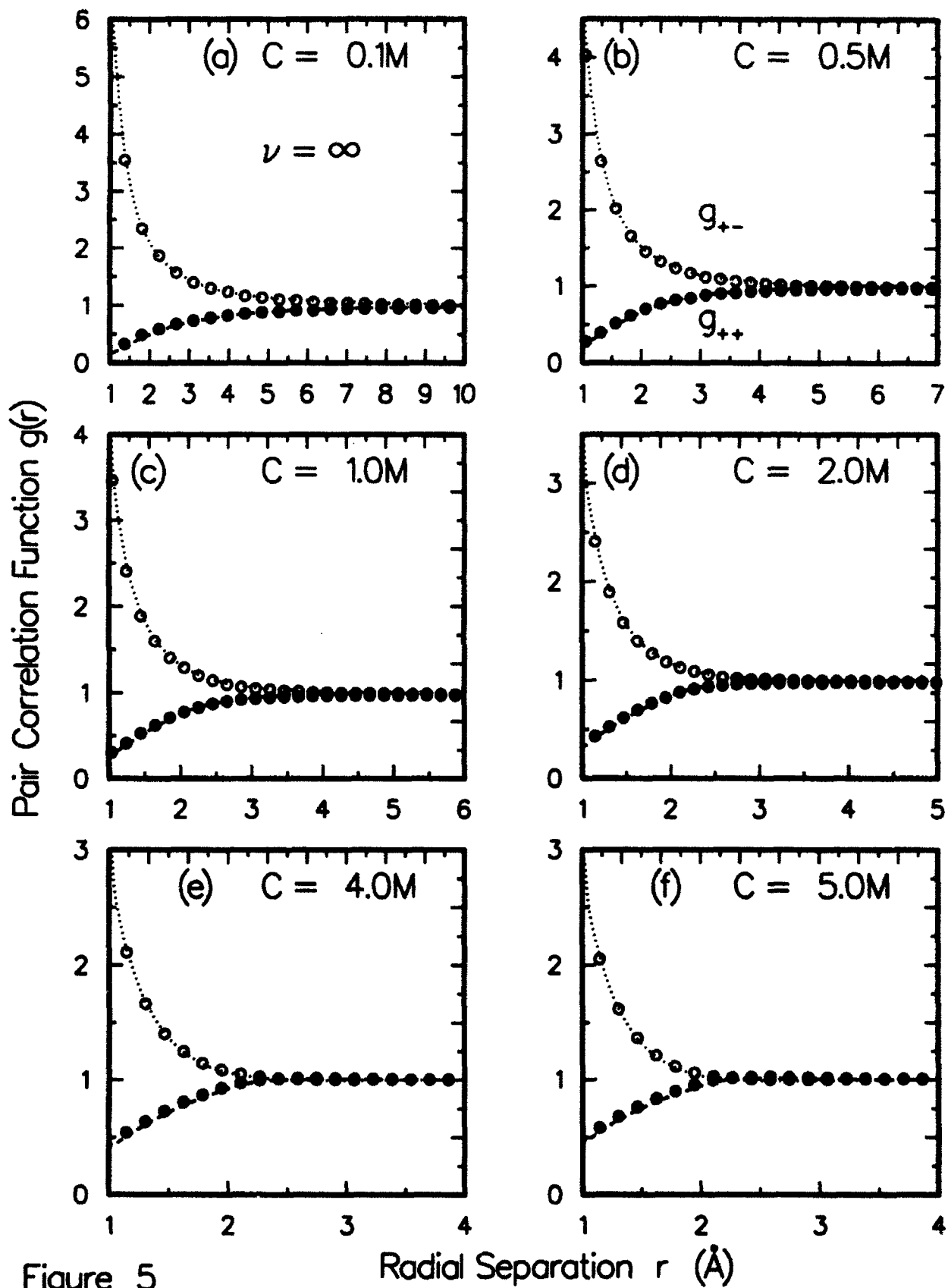


Figure 5

Radial Separation  $r$  (Å)

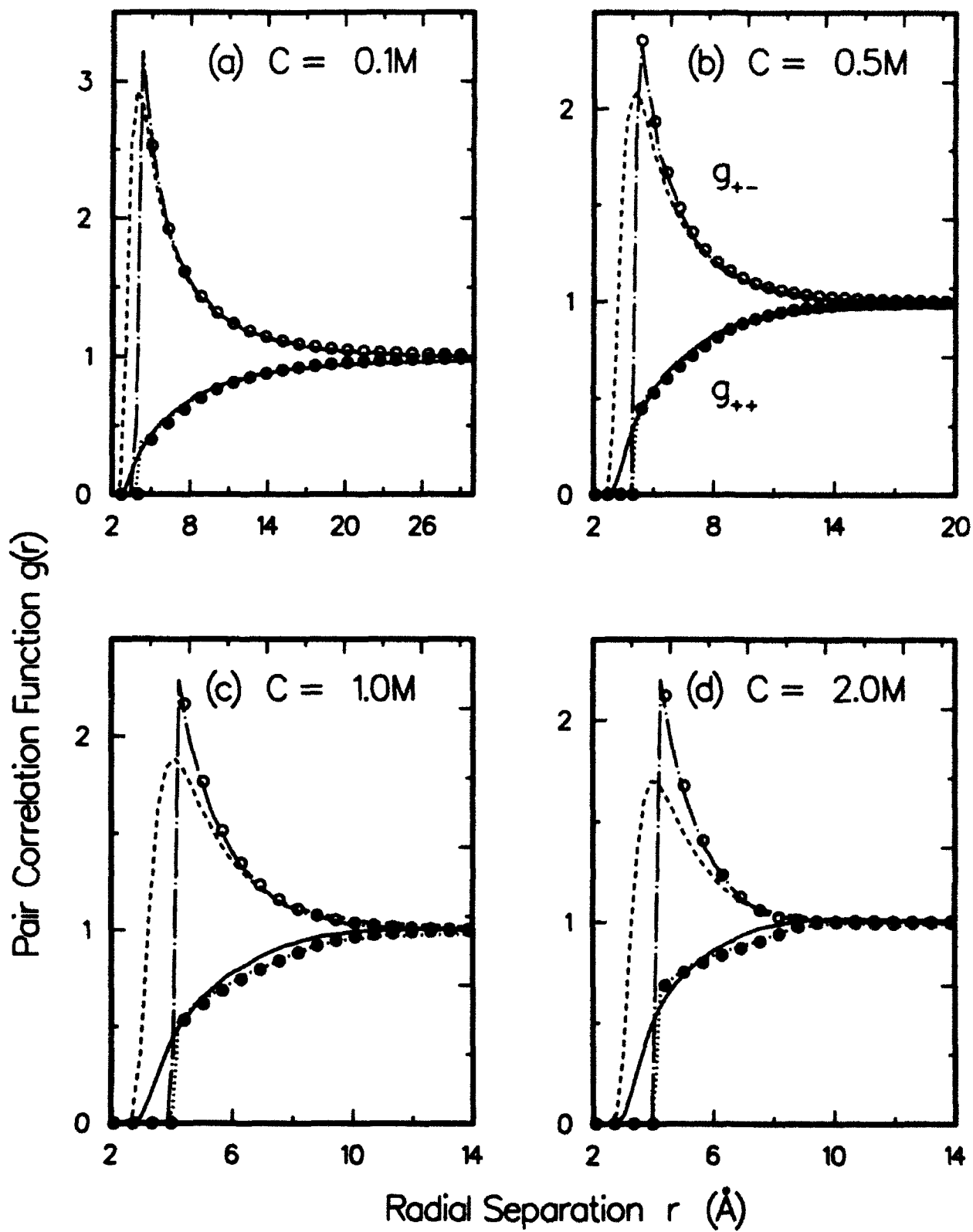


Figure 6

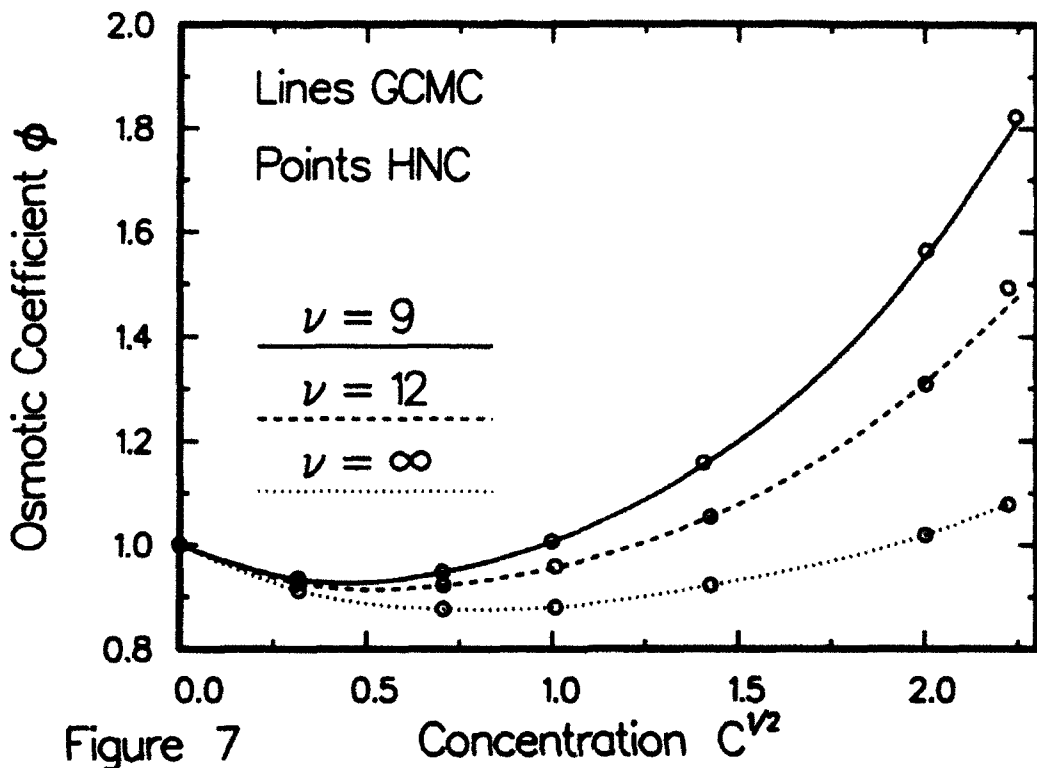


Figure 7

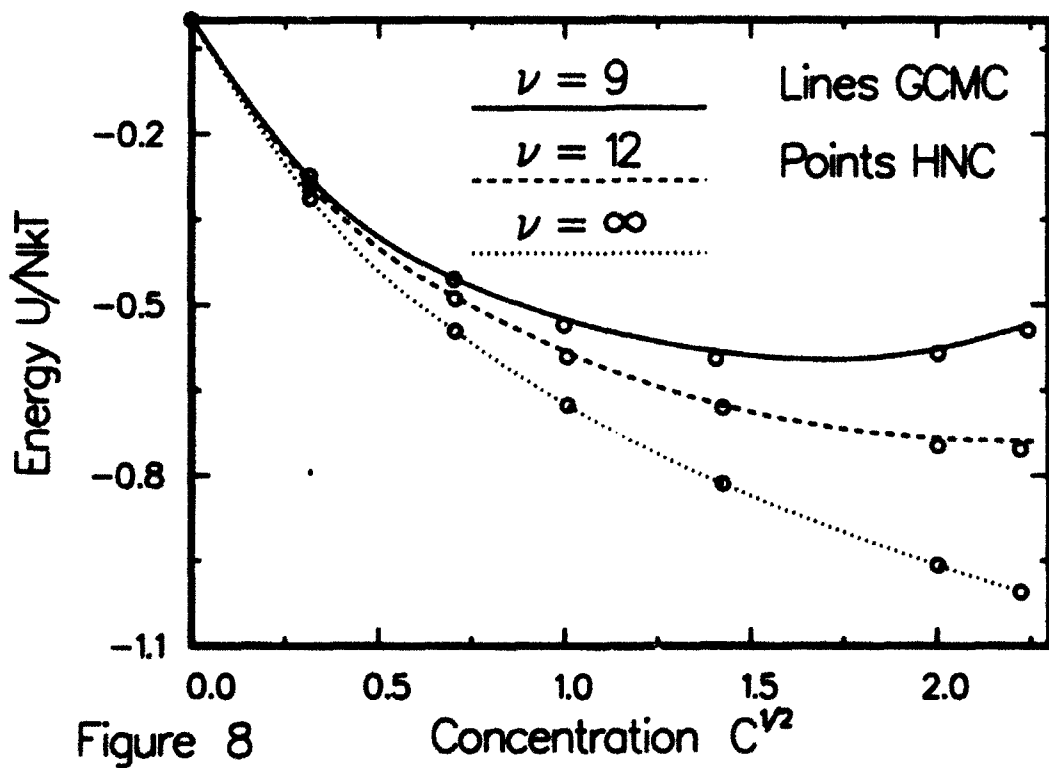


Figure 8

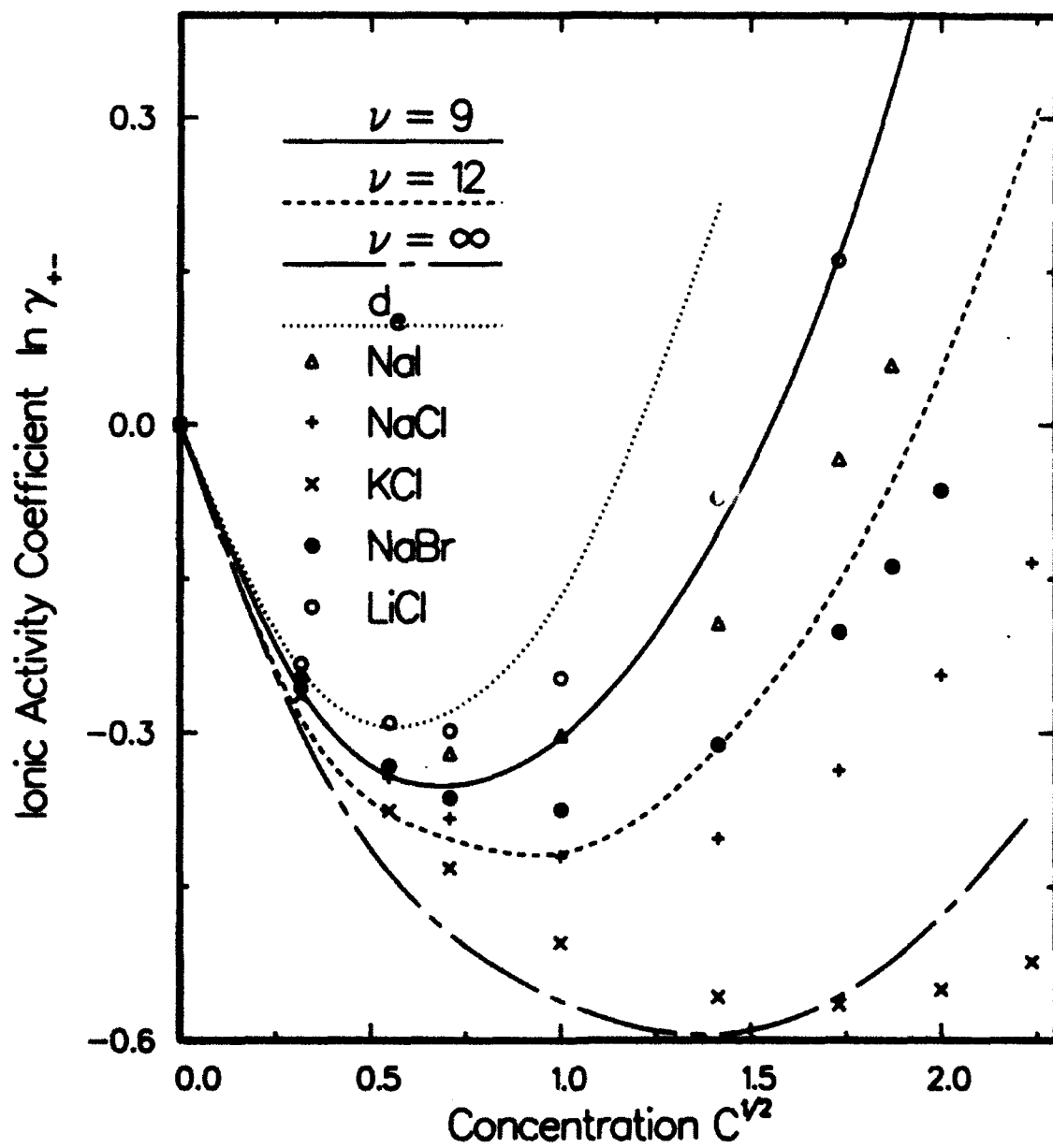


Figure 9